Three-Phase Inverter Modeling using Multifrequency Averaging with Third Harmonic Injection

Xiao Liu, Aaron M. Cramer
Department of Electrical and Computer Engineering
University of Kentucky
Lexington, Kentucky
Email: xiao.liu@uky.edu, aaron.cramer@uky.edu

***Abstract*—Models of converters based on averaging have been used widely with numerous benefits. Multifrequency averaging (MFA) model can predict both the fundamental and switching behavior of converters and has the faster simulation run times associated with average-value models. Third harmonic injection is commonly used in the modulation signal for three-phase inverters to increase the inverter maximum output voltage while avoiding overmodulation. Herein, an MFA model for three-phase pulse width modulation inverters with third harmonic injection is proposed. The quasi-Fourier-series representation of the switching functions with third harmonic injection is necessary for constructing three-phase inverter MFA model. The third harmonic injection does not change the fundamental and third harmonic components of the state variables in a balanced three-phase system, but it changes the higher-order harmonics. As a result, the quasi-Fourier-series representation of the switching functions for three-phase inverters with third harmonic injection must include the third harmonics. The proposed MFA model is demonstrated in simulation, and the simulation results show that this model has high accuracy (including the switching behavior) and fast run times.**

I. Introduction

Three-phase pulse width modulation (PWM) inverters have been widely used in motor drives, renewable energy integration, and other applications. Third harmonic injection is used in the modulation signal for the three-phase inverters to increase the inverter maximum output voltage while avoiding overmodulation, which results in undesirable low-frequency harmonics. Third harmonic injection also can be used to reduce the output current harmonics [1].

Mutifrequency averaging (MFA) is a generalized averaging method that uses a quasi-Fourier-series (QFS) representation of waveforms in order to represent both the fundamental behavior and the switching harmonics. This idea has been developed broadly [2]–[5] with wide application in dc-dc converters. In the MFA model for inverters with sinusoidal modulation signal, the switching functions are represented using two frequencies: the frequency of the sinusoidal modulation signal and the switching frequency associated with the carrier signal. Third harmonic injection does not change the fundamental component of the state variables in a balanced three-phase system, but it changes the higher-order harmonics. As a result, the QFS representation of the switching functions for three-phase inverter with third harmonic injection must include the third harmonics.

Herein, the QFS representation for the switching functions of three-phase PWM inverters with third-harmonic injection is provided. This representation is used to construct an MFA model of three-phase inverters with third-harmonic injection. In the proposed MFA model, the state variables are represented using the fundamental and third harmonic components of the modulation signal, the components corresponding to multiples of the switching frequency and the sideband components of multiples of the switching frequency. At the steady state, the state variable switching ripple magnitude in three-phase inverters changes for each switching period. The sideband components of multiples of the switching frequency cause such variations in the state variable switching ripple magnitude. The sideband components can be included in the MFA model for three-phase inverters. The proposed model is demonstrated in simulation and found to accurately predict both the fundamental and the switching behavior of the three-phase inverter. Furthermore, since the proposed MFA model is time invariant, state variables in this model are constant in the steady state and the simulation speed of the MFA model is significantly faster than that of the detailed model. The contributions of this work are (1) the QFS representation of the switching function of three-phase PWM inverters with third harmonic injection, (2) the proposal of an MFA model for PWM three-phase inverters with third harmonic injection, and (3) the demonstration of the proposed MFA model in simulation.

The remainder of this paper is organized as follows. The QFS representation of the switching function of three-phase PWM inverters with third harmonic injection is described in Section II. In Section III, the MFA model for three-phase inverters is proposed. The proposed three-phase inverter MFA model is compared with a detailed model in Section IV. Finally, conclusions are drawn in Section V.

978-1-5090-0737-0/16/$31.00 ©2016 IEEE

II. Multifrequency Averaging Model

Herein, the QFS representation of the state variables in three-phase PWM inverters with third harmonic injection is studied. By assuming the modulation signal is a sinusoidal waveform with third harmonic injection, the modulation signal can be expressed by

$$m(t) = m_1 \cos(\bar{\omega}t + \bar{\phi}_0) + m_3 \cos(3\bar{\omega}t + \bar{\phi}_{30}), \quad (1)$$

where $\bar{\omega}$ is the angular frequency of the modulation signal, m_1 and m_3 are the magnitude of the fundamental modulation signal and third harmonic injection, respectively, and $\bar{\phi}_0$ and $\bar{\phi}_{30}$ are the phase angle of the fundamental modulation signal and third harmonic injection, respectively. The instantaneous switch duty cycle can be expressed as

$$D = \frac{1}{2}(m(t) + 1). \quad (2)$$

The instantaneous switching function is generated by comparing the switch duty cycle D with the double-edge triangular carrier signal $c(t)$ as in the following relationship:

$$q(t) = \begin{cases} 1, & D \geq c(t) \\ 0, & \text{otherwise} \end{cases}. \quad (3)$$

The general periodic switching function for constant duty cycle D can be expressed as the following Fourier series:

$$q(t) = D + \frac{2}{\pi} \sum_{n=1}^{\infty} \frac{\sin(n\pi D)}{n} \cos(n\hat{\omega}t + n\hat{\phi}), \quad (4)$$

where $\hat{\omega}$ is the angular frequency of switching function and $\hat{\phi}$ is the phase angle of the switching function. In [2], it states that the same switching function expression can be used with the time-varying duty cycle for the slowly varying duty cycle. It is assumed that the modulation signal changes more slowly than the switching signal. By substituting (1) and (2) into (4), it can be shown that the general QFS representation of the switching function for sinusoidal modulation signal with third harmonic injection can be given by

$$\begin{aligned} q(t) = {} & q_{0,0} + q_{0,1c}\cos(\bar{\omega}t) + q_{0,1s}\sin(\bar{\omega}t) + q_{0,3c}\cos(3\bar{\omega}t) \\ & + q_{0,3s}\sin(3\bar{\omega}t) + \sum_{n=1}^{\infty}\sum_{i=-\infty}^{\infty} q_{n,ic}\cos(n\hat{\omega}t + i\bar{\omega}t) \\ & + \sum_{n=1}^{\infty}\sum_{i=-\infty}^{\infty} q_{n,is}\sin(n\hat{\omega}t + i\bar{\omega}t), \end{aligned} \quad (5)$$

where

$$q_{0,0} = \frac{1}{2} \quad (6)$$

$$q_{0,1c} = \frac{1}{2} m_1 \cos(\bar{\phi}_0) \quad (7)$$

$$q_{0,1s} = -\frac{1}{2} m_1 \sin(\bar{\phi}_0) \quad (8)$$

$$q_{0,3c} = \frac{1}{2} m_3 \cos(\bar{\phi}_{30}) \quad (9)$$

$$q_{0,3s} = -\frac{1}{2} m_3 \sin(\bar{\phi}_{30}) \quad (10)$$

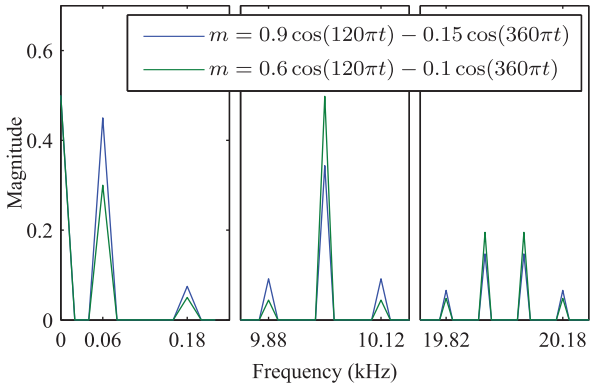

Fig. 1. Discrete Fourier transform of switching functions

$$\begin{aligned} q_{n,ic} = {} & \sum_{j=-\infty}^{\infty} \frac{2}{n\pi} J_{i-3j}\left(\frac{n\pi m_1}{2}\right) J_j\left(\frac{n\pi m_3}{2}\right) \\ & \sin\left(\frac{(n+i-2j)\pi}{2}\right) \\ & \cos\left(n\hat{\phi} + (i-3j)\bar{\phi}_0 + j\bar{\phi}_{30}\right) \end{aligned} \quad (11)$$

$$\begin{aligned} q_{n,is} = {} & -\sum_{j=-\infty}^{\infty} \frac{2}{n\pi} J_{i-3j}\left(\frac{n\pi m_1}{2}\right) J_j\left(\frac{n\pi m_3}{2}\right) \\ & \sin\left(\frac{(n+i-2j)\pi}{2}\right) \\ & \sin\left(n\hat{\phi} + (i-3j)\bar{\phi}_0 + j\bar{\phi}_{30}\right) \end{aligned} \quad (12)$$

The function $J_y(x)$ is the Bessel function of the first kind of integer order y. The analyses of the harmonic spectrum of PWM waveforms with third harmonic injection can also be found in [6].

Discrete Fourier transformations are used to find the magnitudes of the components of the switching functions. Two switching functions are generated by comparing a 10-kHz carrier signal with two different a-phase 60-Hz modulation signals which are sampled at 30 MHz. The magnitude of the third harmonic injection m_3 is set to $-m_1/6$ to allow for a wider voltage range without overmodulation. Fig. 1 shows the most important components of the switching functions. It can be seen that all harmonic amplitudes of the switching functions except for the dc component amplitude change when the magnitudes of the fundamental modulation signal and third harmonic injection change. When the sum $n + i$ is even, the $\sin((n+i-2j)\pi/2)$ terms in (11) and (12) are equal to zero, resulting in vanishing of the corresponding components of the switching functions. So, there are no 9.94 kHz, 10.06 kHz, 20 kHz, 19.88 kHz and 20.12 kHz harmonics in Fig. 1. The harmonic amplitudes shown in Fig. 1 can also be calculated by using (5)–(12).

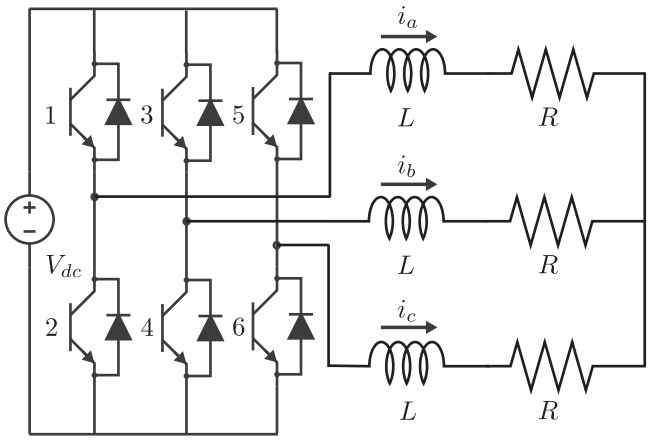

Fig. 2. Three-phase inverter

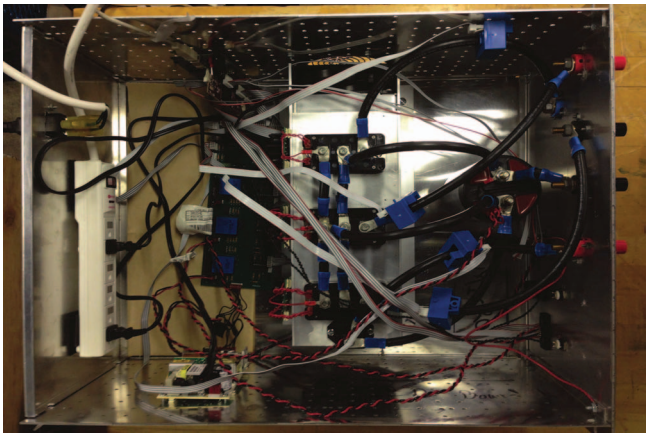

Fig. 3. Three-phase inverter prototype

All of the state variables of the PWM inverter can be expressed using a QFS representation similar to that of the switching function. The instantaneous state variables can be approximated by the QFS representation as

$$x(t) \approx \mathbf{C}(t)\mathbf{x}, \tag{13}$$

where

$$\mathbf{x} = [x_{0,0}\ x_{n_1,i_1c}\ x_{n_1,i_1s}\ \ldots\ x_{n_o,i_oc}\ x_{n_o,i_os}]^{\mathrm{T}}, \tag{14}$$

$$\mathbf{C}(t) = \begin{bmatrix} 1 \\ \cos(n_1\hat{\omega}t + i_1\bar{\omega}t) \\ \sin(n_1\hat{\omega}t + i_1\bar{\omega}t) \\ \vdots \\ \cos(n_o\hat{\omega}t + i_o\bar{\omega}t) \\ \sin(n_o\hat{\omega}t + i_o\bar{\omega}t) \end{bmatrix}^{\mathrm{T}}, \tag{15}$$

$x_{0,0}$, x_{n_1,i_1c}, x_{n_1,i_1s}, $\ldots$ x_{n_o,i_oc} and x_{n_o,i_os} are index-0, index-n_1i_1c, index-n_1i_1s, $\ldots$ index-n_oi_oc, and index-n_oi_os QFS coefficients of the Fourier series of state variables, respectively, and n_k is the order of the kth selected $\hat{\omega}$ component and i_k is the corresponding order of kth selected $\bar{\omega}$ component for $k \in \{1, 2, \ldots o\}$. It can be seen that the average vector $\mathbf{x}$ is constructed by the QFS coefficients and has $2o+1$ elements.

III. Inverter Multifrequency Averaging Model

The three-phase grid-tie inverter is shown in Fig. 2. For each branch, the switching function is equal to 1 when the corresponding upper switch is on and is equal to 0 when the corresponding lower switch is on. The state equations for the detailed model are given by

$$\frac{di_a(t)}{dt} = \frac{V_{dc}}{L}\left(\frac{2}{3}q_a(t) - \frac{1}{3}q_b(t) - \frac{1}{3}q_c(t)\right) - \frac{R}{L}i_a(t) \tag{16}$$

$$\frac{di_b(t)}{dt} = \frac{V_{dc}}{L}\left(\frac{2}{3}q_b(t) - \frac{1}{3}q_a(t) - \frac{1}{3}q_c(t)\right) - \frac{R}{L}i_b(t) \tag{17}$$

$$\frac{di_c(t)}{dt} = \frac{V_{dc}}{L}\left(\frac{2}{3}q_c(t) - \frac{1}{3}q_a(t) - \frac{1}{3}q_b(t)\right) - \frac{R}{L}i_c(t). \tag{18}$$

where $q_a(t)$, $q_b(t)$ and $q_c(t)$ are the three-phase switching functions. By using average vectors instead of instantaneous values of the state variables and switching functions, (16)–(18) become

$$\frac{d\mathbf{i}_a}{dt} = \frac{V_{dc}}{L}\left(\frac{2}{3}\mathbf{q}_a - \frac{1}{3}\mathbf{q}_b - \frac{1}{3}\mathbf{q}_c\right) - \left(\mathbf{T} + \frac{R}{L}\mathbf{I}\right)\mathbf{i}_a \tag{19}$$

$$\frac{d\mathbf{i}_b}{dt} = \frac{V_{dc}}{L}\left(\frac{2}{3}\mathbf{q}_b - \frac{1}{3}\mathbf{q}_a - \frac{1}{3}\mathbf{q}_c\right) - \left(\mathbf{T} + \frac{R}{L}\mathbf{I}\right)\mathbf{i}_b \tag{20}$$

$$\frac{d\mathbf{i}_c}{dt} = \frac{V_{dc}}{L}\left(\frac{2}{3}\mathbf{q}_c - \frac{1}{3}\mathbf{q}_a - \frac{1}{3}\mathbf{q}_b\right) - \left(\mathbf{T} + \frac{R}{L}\mathbf{I}\right)\mathbf{i}_c, \tag{21}$$

where $\mathbf{q}_a$, $\mathbf{q}_b$ and $\mathbf{q}_c$ are the average vectors of the three-phase switching functions, and $\mathbf{i}_a$, $\mathbf{i}_b$ and $\mathbf{i}_c$ are the average vectors of the three-phase inductor currents, $\mathbf{I}$ is the identity matrix and $\mathbf{T}$ is a $(2o+1)\times(2o+1)$ matrix that is constructed such that all elements are zero except for the $(2k, 2k+1)$ elements with values $n_k\hat{\omega} + i_k\bar{\omega}$ and the $(2k+1, 2k)$ elements with values $-(n_k\hat{\omega} + i_k\bar{\omega})$ for $k \in \{1, 2, \ldots o\}$.

To achieve the maximum output voltage without overmodulation [6], the three-phase modulation signals with third harmonic injection are given by

$$m_a = m_1\cos(\bar{\omega}t + \bar{\phi}_a) - \frac{m_1}{6}\cos(3\bar{\omega}t + 3\bar{\phi}_a) \tag{22}$$

$$m_b = m_1\cos(\bar{\omega}t + \bar{\phi}_a - \frac{2\pi}{3}) - \frac{m_1}{6}\cos(3\bar{\omega}t + 3\bar{\phi}_a) \tag{23}$$

$$m_c = m_1\cos(\bar{\omega}t + \bar{\phi}_a + \frac{2\pi}{3}) - \frac{m_1}{6}\cos(3\bar{\omega}t + 3\bar{\phi}_a). \tag{24}$$

where $\bar{\phi}_a$ is the phase angle of the a-phase fundamental modulation signal. It is noted that if such three-phase modulations are compared with the same PWM carrier, the components corresponding to multiples of the switching frequency (i.e., $q_{n,0c}$ and $q_{n,0s}$) for the three-phase switching functions are equal. These components can be canceled in (19)-(21). As a result, no components corresponding to multiples of the switching frequency exist in the inductor currents. It can be seen from (6)-(10) that the magnitudes of the fundamental and third harmonic components for three-phase switching functions are equal to each other. From (11) and (12), the

magnitudes of high frequency components can be given by

$$\sqrt{q_{n,ic}^2 + q_{n,is}^2} = \sum_{j=-\infty}^{\infty} \frac{2}{n\pi} J_{i-3j}\left(\frac{n\pi m_1}{2}\right) J_j\left(\frac{n\pi m_3}{2}\right) \sin\left(\frac{(n+i-2j)\pi}{2}\right), \quad (25)$$

which means that the magnitudes of high frequency components of three-phase switching functions on the same frequency are also equal in the balanced system. Therefore, three-phase switching functions have the same significant harmonic components.

IV. Simulation Results

In order to examine the proposed inverter MFA model, simulation of the three-phase inverter is discussed in this section. The model is simulated by the ode32tb Simulink solver with a default relative tolerance of 10^{-3} in MATLAB 2013a. The Bessel function of the first kind is implemented using the MATLAB interpreter. The simulation time for each simulation study is 2 s. The run time of the simulation is reported as the mean run time over 100 simulations. The initial values of the state variables in the simulation are equal to the corresponding steady state values.

The structure of the three-phase inverter for the simulation is shown in Fig. 2. The parameters of the three-phase inverter are listed in the Table I. A modulation signal step change is considered. Two configurations of three-phase inverter MFA model are studied. In Configuration 1, the switching functions and state variables of the MFA model are represented using 60-Hz components and 9.88-kHz and 10.12-kHz components that are sidebands to the 10-kHz switching frequency. In Configuration 2, the switching functions and state variables of the MFA model are represented using not only all of components in Configuration 1 but also 19.94-kHz and 20.06-kHz components that are sidebands to double the switching frequency. Two configurations are compared with a detailed model that models every switching action. From (5)–(12), it is can be seen that the coefficients of the switching functions for a given harmonic are an infinite sum except for the dc, fundamental, and third harmonic injection components. However, these coefficients are approximated by several terms. In particular, the 9.88-kHz component is approximated by the sum of terms with $j \in \{-1, 0\}$. The 10.12-kHz component is approximated by the sum of terms with $j \in \{0, 1\}$. The 19.94-kHz and 20.06-kHz components are approximated by the sum of terms with $j \in \{-1, 0, 1\}$. Because $J_{-y}(x) = (-1)^y J_y(x)$, only four Bessel function evaluations are needed for Configuration 1 of the MFA model and nine Bessel function evaluations are needed for Configuration 2 of the MFA model. The magnitudes of harmonic components of a-phase switching function given by the approximation and the fast Fourier transform (FFT) are compared in Table II. The sampling frequency of a-phase switching function for the FFT is 30 MHz. As mentioned in Section III, the magnitudes of harmonic components of three-phase switching functions on same frequency are equal to each other. So, the magnitudes of harmonic components for b-phase and c-phase switching functions given by the approximation and the FFT have the same results. From Table II, it can be seen that the approximations of QFS coefficients have high accuracy.

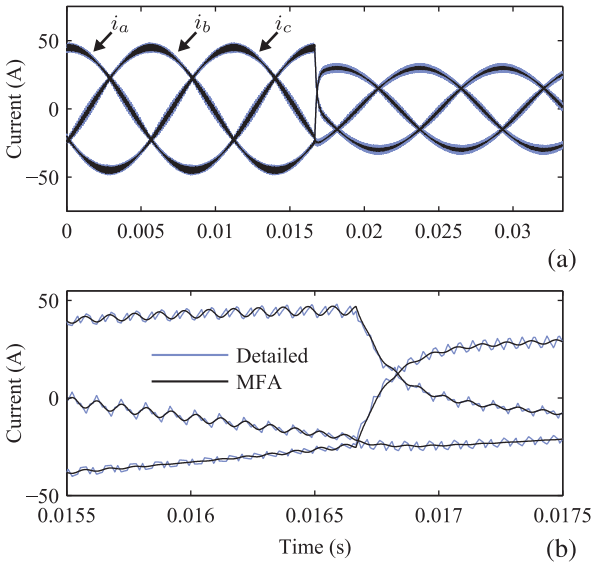

Fig. 4. Configuration 1 three-phase inverter inductor currents

Three-phase inductor currents during the first two fundamental periods predicted by the detailed model and by Configuration 1 of the MFA model are shown in Fig. 4 (a). Three-phase inductor currents near the step modulation signal change are shown in Fig. 4 (b). From Fig. 4, it can be seen that the inductor currents predicted by Configuration 1 of the MFA model match the inductor currents predicted by the detailed model during both steady-state and transient conditions.

Three-phase inductor currents during the first two fundamental periods predicted by the detailed model and by Configuration 2 of the MFA model are shown in Fig. 5 (a). Three-phase inductor currents near the step modulation signal change are shown in Fig. 5 (b). From Fig. 5, it can be seen that the inductor currents predicted by Configuration 2 of the MFA model also match the inductor currents predicted by the detailed model.

It can be seen that the accuracy of Configuration 2 of the MFA model is increased (with respect to Configuration 1) by including more sideband components. Furthermore, the accuracy of Configuration 1 of the MFA model noticeably suffers after the modulation signal step change (e.g., i_c at approximately 17 ms). This decrease in accuracy can be understood from Fig. 1. In Fig. 1, the magnitudes of the 9.88-kHz and 10.12-kHz sideband components are smaller than the magnitudes of the 19.94-kHz and 20.06-kHz sideband components when the magnitude of the fundamental component m_1 is equal to 0.6 (as it is after the step change).

The run times of the detailed model and both configurations

TABLE I
THREE-PHASE INVERTER SIMULATION PARAMETERS

Input voltage, V_{dc}	220 V
Inductance of L filter, L	0.276 mH
Load resistance, R	2.2 Ω
Switching frequency, $\hat{f}$	10 kHz
Phase angle of switching function, $\hat{\phi}$	0 rad
Modulation signal frequency, $\bar{f}$	60 Hz
Initial modulation signal, $m_a(t)$ (initial)	$0.9\cos(\bar{\omega}t) - 0.15\cos(3\bar{\omega}t)$
Final modulation signal, $m_a(t)$ (final)	$0.6\cos(\bar{\omega}t + \pi/2) - 0.1\cos(3\bar{\omega}t + 3\pi/2)$
Modulation signal step time	16.7 ms

TABLE II
MAGNITUDE OF A-PHASE SWITCHING FUNCTION HARMONICS FROM APPROXIMATION AND FAST FOURIER TRANSFORM

Harmonic frequency			9.88 kHz	10.12 kHz	19.94 kHz	20.06 kHz
Harmonic magnitude	$m_a(t)$ (initial)	FFT	0.0917	0.0917	0.1472	0.1472
		Approximation	0.0917	0.0917	0.1475	0.1475
	$m_a(t)$ (final)	FFT	0.0442	0.0442	0.1953	0.1953
		Approximation	0.0442	0.0442	0.1953	0.1953

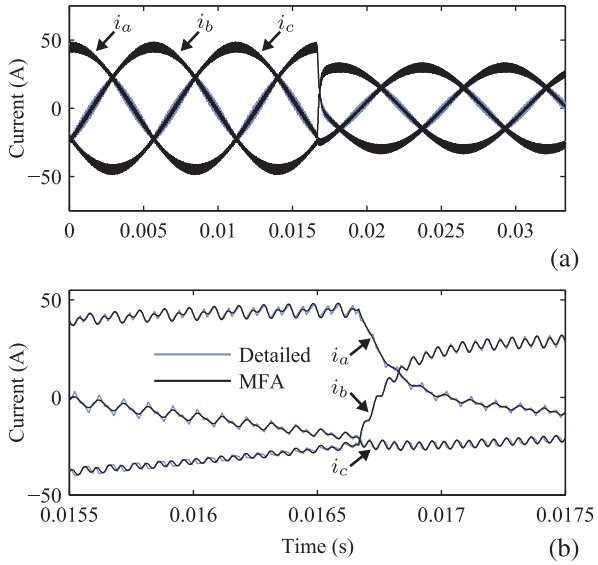

Fig. 5. Configuration 2 three-phase inverter inductor currents

of the MFA model are listed in Table III. It can be seen that the average simulation run time of detailed model is more than 67 times larger than that of Configuration 1 of the MFA model. The average simulation run time of detailed model is more than 35 times larger than that of Configuration 2 of the MFA model. To compare the accuracy of different configurations of the MFA model, the mean deviation between the inductor current of the MFA model and that of the detailed model is defined by

$$\frac{1}{T}\int_0^T \sqrt{(i_{MFA}(t) - i_{detailed}(t))^2}, \tag{26}$$

where T is the simulation time, i_{MFA} is the inductor current predicted by the MFA model and $i_{detailed}$ is the inductor current predicted by the detailed model. The mean deviations

TABLE III
THREE-PHASE INVERTER SIMULATION RUN TIME

Model	Run time (ms)
Detailed	5162
Configuration 1	76
Configuration 2	140

TABLE IV
MEAN DEVIATION OF THREE-PHASE INVERTER INDUCTOR CURRENTS

Model	Inductor current mean deviation (A)		
	a phase	b phase	c phase
Configuration 1	1.131	1.131	1.131
Configuration 2	0.482	0.482	0.482

of three-phase inductor currents are listed in Table IV. It can also be seen that the Configuration 2 of the MFA model has better accuracy than Configuration 1 of the MFA model. So, there is a trade-off between the simulation speed and accuracy in the MFA model for three-phase inverters.

V. CONCLUSION

Achieving the proper balance between accuracy and computational efficiency is necessary in any simulation application. Models based on averaging have been used widely with numerous benefits. MFA techniques have been used to predict both average and switching behavior of converters while retaining the faster simulation speed associated with average-value models. Herein, an MFA model for three-phase PWM inverters with third harmonic injection is proposed. The QFS representation of the switching functions with third harmonic injection are necessary for constructing three-phase inverter MFA model. The QFS representation of the switching functions includes fundamental components, third harmonic components, components corresponding to multiples of the switching frequency and sideband components of multiples of the switching frequency. Due to the third harmonic com-

ponents and components corresponding to multiples of the switching frequency do not exist in the state variables of three-phase inverters, the sideband components of of multiples of the switching frequency cause the variations in inductor current ripple magnitude. The accuracy of the MFA model of three-phase inverter can be improved by including more sideband components in average vectors, but the simulation run time will increase. The simulation results show the MFA model have high accuracy and simulation run times that are significantly faster than those associated with detailed models.

REFERENCES

[1] A. Eltamaly, "A modified harmonics reduction technique for a three-phase controlled converter," *IEEE Trans. Ind. Electron.*, vol. 55, no. 3, pp. 1190–1197, Mar. 2008.

[2] V. Caliskan, G. C. Verghese, and A. Stanković, "Multifrequency averaging of DC/DC converters," *IEEE Trans. Power Electron.*, vol. 14, no. 1, pp. 124–133, Jan. 1999.

[3] S. Sanders, J. Noworolski, X. Liu, and G. C. Verghese, "Generalized averaging method for power conversion circuits," *IEEE Trans. Power Electron.*, vol. 6, no. 2, pp. 251–259, Apr. 1991.

[4] J. Mahdavi, A. Emaadi, M. Bellar, and M. Ehsani, "Analysis of power electronic converters using the generalized state-space averaging approach," *IEEE Trans. Circuits Syst. I*, vol. 44, no. 8, pp. 767–770, Aug. 1997.

[5] H. Behjati, L. Niu, A. Davoudi, and P. Chapman, "Alternative time-invariant multi-frequency modeling of PWM DC-DC converters," *IEEE Trans. Circuits Syst. I, Reg. Papers*, vol. 60, no. 11, pp. 3069–3079, Nov. 2013.

[6] D. Holmes and T. Lipo, *Pulse Width Modulation for Power Converters: Principles and Practice*. Piscataway, NJ: Wiley-IEEE Press, 2003.